# Coordinated Reversal of Flagellar Motors on a Single *Escherichia coli* Cell

Shun Terasawa,[†△] Hajime Fukuoka,[†‡△] Yuichi Inoue,[†‡] Takashi Sagawa,[†] Hiroto Takahashi,[‡] and Akihiko Ishijima[†‡*]

[†]Graduate School of Life Sciences and [‡]Institute of Multidisciplinary Research for Advanced Materials, Tohoku University, Aoba-ku, Sendai, Japan

ABSTRACT An *Escherichia coli* cell transduces extracellular stimuli sensed by chemoreceptors to the state of an intracellular signal molecule, which regulates the switching of the rotational direction of the flagellar motors from counterclockwise (CCW) to clockwise (CW) and from CW back to CCW. Here, we performed high-speed imaging of flagellar motor rotation and show that the switching of two different motors on a cell is controlled coordinatedly by an intracellular signal protein, phosphorylated CheY (CheY-P). The switching is highly coordinated with a subsecond delay between motors in clear correlation with the distance of each motor from the chemoreceptor patch localized at a cell pole, which would be explained by the diffusive motion of CheY-P molecules in the cell. The coordinated switching becomes disordered by the expression of a constitutively active CheY mutant that mimics the CW-rotation stimulating function. The coordinated switching requires CheZ, which is the phosphatase for CheY-P. Our results suggest that a transient increase and decrease in the concentration of CheY-P caused by a spontaneous burst of its production by the chemoreceptor patch followed by its dephosphorylation by CheZ, which is probably a wavelike propagation in a subsecond timescale, triggers and regulates the coordinated switching of flagellar motors.

## INTRODUCTION

Signal transduction systems are conserved in a wide range of living organisms from eukaryotes to prokaryotes (1–4) and are essential processes by which cells respond to chemical and mechanical changes in the environment. Many bacteria, including the peritrichously flagellated *Escherichia coli*, swim by rotating their locomotive organelles called flagella. In response to extracellular stimuli, such as chemicals, pH, or temperature, *E. coli* cells reorient themselves during swimming by changing the rotational direction of their flagellar motors (4). *E. coli* cells swim smoothly when all the flagellar motors rotate counterclockwise (CCW), which causes the left-handed helical flagellar filaments to form a bundle. When one or more of the motors switch to the clockwise (CW) rotation, the bundle is disrupted, and the cells tumble. The cell then swims in a new direction when the normal to semicoiled polymorphic transformation is complete. The cell attains the initial run speed when the motors switch back to CCW, and the filaments rejoin the normal bundle (5).

In bacteria, extracellular chemicals are sensed by chemoreceptors that are localized primarily at one of the cellular poles (4). When chemotactic signals are sensed by their receptors, they modulate the autophosphorylation activity of a histidine protein kinase, CheA, which is associated with their cytoplasmic domain; attractant chemicals inhibit the autophosphorylation activity of CheA, and repellent chemicals appear to increase it (4). The phosphoryl group on CheA is rapidly transferred to a response regulator, CheY. Phosphorylated CheY (CheY-P) binds to the flagellar motor and increases the probability of CW rotation. The functions of proteins involved in chemotaxis and their localization within the cell are relatively well understood. However, it is still uncertain how the cell changes the rotation of its multiple flagella in response to extracellular stimuli or if the switching of their rotational directions is coordinated in some way.

To investigate the regulatory mechanism of multiple flagellar motors by the signal transduction system, we measured the rotation of motors on individual *E. coli* cells simultaneously, using a bead assay and high-speed imaging. The results clearly show that the directional switching of the motors is coordinated, and the timing of the switching is correlated with the distance of the motor from the chemoreceptor patch.

## MATERIALS AND METHODS

### *E. coli* strains and plasmids

The *E. coli* strains and plasmids are listed in Table S1 in the Supporting Material. All the *E. coli* strains were derived from the K12 strain RP437 [*thr leu his metF eda rpsL thi ara lacY xyl tonA tsx*], which is wild-type for chemotaxis (6). The deletion of the *che* genes and the replacement of the wild-type *fliC* gene with the *fliC-sticky* gene (7) were carried out using the λ red recombinase and tetracycline sensitivity selection method (8,9). LB broth (1% bactotryptone, 0.5% yeast extract, 0.5% NaCl) was used for culture growth, transformations, and plasmid isolation. Tryptone broth (TB) (1% bactotryptone, 0.5% NaCl) was used to grow cells for measurements of motor rotation. For the measurement of multiple flagellar motors on cells expressing GFP-CheW (the N-terminal GFP-fusion of CheW), EFS031 cells harboring pTH2300 and pBAD24-GFP-CheW were grown in TB containing 30 μM IPTG, 0.002% arabinose, 25 μg/mL chloramphenicol, and 50 μg/mL ampicillin at 30°C for 5 h. For the measurement of cells

*Submitted December 22, 2010, and accepted for publication March 14, 2011.*

△Shun Terasawa and Hajime Fukuoka contributed equally to this work.

*Correspondence: ishijima@tagen.tohoku.ac.jp

Editor: Robert Nakamoto.



0006-3495/11/05/2193/8 $2.00

doi: 10.1016/j.bpj.2011.03.030

without GFP-CheW, EFS031 cells harboring pTH2300 were grown in TB containing 30 $\mu$M IPTG and 25 $\mu$g/mL chloramphenicol at 30°C for 5 h.

For measurements of cells producing constitutively active CheY, EFS031 cells harboring pTH2300 and pAH115 were grown at 30°C for 5 h in TB containing 30 $\mu$M IPTG, 25 $\mu$g/mL chloramphenicol, and 50 $\mu$g/mL ampicillin. For the measurement of *cheZ*-deleted cells, EFS032 cells harboring pTH2300 were grown in TB containing 30 $\mu$M IPTG and 25 $\mu$g/mL chloramphenicol at 30°C for 5 h. To investigate complementation by a CheZ expressed from a plasmid, EFS032 cells harboring pTH2300 and pFSZ1 were grown in TB containing 30 $\mu$M IPTG, 0.002% arabinose, 25 $\mu$g/mL chloramphenicol, and 50 $\mu$g/mL ampicillin at 30°C for 5 h. For the measurement of artificial filamentous cells, EFS031 cells harboring pTH2300 and pBAD24-GFP-CheW were grown in TB containing 30 $\mu$M IPTG and 0.002% arabinose at 30°C for 3 h. Cephalexin was added to a final concentration of 50 $\mu$g/mL, and the cells were grown for an additional 2 h at 30°C.

## Measurement of flagellar rotation

Cells were suspended in 10 NaMB (10 mM Potassium phosphate buffer at pH 7.0; 0.1 mM EDTA-2K, pH 7.0; and 10 mM NaCl, 75 mM KCl) and the cell suspensions were loaded into the space between 18 × 18 and 24 × 50 mm coverslips with a spacer and incubated for 10 min to allow the cells to attach to the coverslip. The space between the coverslips was gently perfused with additional 10 NaMB to remove the remaining unattached cells. A suspension of polystyrene beads, diameter 0.5 $\mu$m, was injected, and the mixture was incubated for 10 min to allow the beads to attach to the flagellar filaments. The space between coverslips was gently perfused again with additional 10 NaMB to remove unattached beads.

The rotational motions of the beads were observed under phase-contrast microscopy (IX71; Olympus, Tokyo, Japan) and recorded with a high-speed charge-coupled device (CCD) camera (model No. IPX-VGA210LMCN; Imperx, Boca Raton, FL) at 1250 frames/s. Phase-contrast images of each bead were cropped to the proper pixel-size (11 × 11 – 13 × 13 pixels) by the free software ImageJ (http://rsb.info.nih.gov/ij/). Phase-contrast images of each bead were fitted by a two-dimensional Gaussian function, and the position, angular velocity, and rotational direction of the bead were calculated using analytical programs written in-house using Labview 2009 (National Instruments, Austin, TX).

The spatial resolution of our measurement system was confirmed to be 1 nm, which corresponds to an angular resolution of 0.3°. To observe the GFP-CheW, a blue laser beam (Sapphire 488-20-SV; Coherent, Hercules, CA) was focused on the back focal plane of the objective lens (UPlanFl 40× NA 0.75 Ph2; Olympus). The fluorescence images were recorded with the high-speed CCD camera at two frames/s after measuring the rotational motion of the beads.

## Preparation of data set for correlation analysis

To analyze the correlation in the switching between flagellar motors, the rotational speed was classified into three states by the following procedure. The time-trace of the rotational speed was filtered by the Chug-Kennedy filtering algorithm (C-K filter) (10), using an analytical window of 100 data-points and a weight of 10 (see Fig. S1 *A*, *middle trace*, in the Supporting Material). From the trace of the rotational speed run through the C-K filter, a rotational speed of >20 Hz, between ±20 Hz, and <−20 Hz were assigned as CCW rotation (+1), pause (0), and CW rotation (−1), respectively (see Fig. S1 *A*, *bottom trace*). The resultant traces of rotational direction against time were then subjected to the correlation analysis.

## Correlation analysis

The correlation analysis was performed by applying Eq. 1 to the time traces of the rotational directions between two flagellar motors,

$$Z(\tau) = \frac{\frac{1}{N}\sum_{t=1}^{N}\left[x(t) \times y(t+\tau) - \overline{x(t)} \times \overline{y(t)}\right]}{\sqrt{\frac{1}{N}\sum_{t=1}^{N}\left[x(t) - \overline{x(t)}\right]^2} \times \sqrt{\frac{1}{N}\sum_{t=1}^{N}\left[y(t) - \overline{y(t)}\right]^2}}, \quad (1)$$

where $Z$ is the function used for the correlation analysis, $t$ is time, $\tau$ is the time difference, $N$ is the total number of sampling points, and $x(t)$ and $y(t)$ are the time traces of the rotational directions of two motors, respectively. In cells producing GFP-CheW, this function was applied based on the motor closer to the fluorescent patch at one of the cell poles. We analyzed motors separated by <2 $\mu$m (cells were <3 $\mu$m long). All correlations ($Z(\tau)$) were calculated ($-1 \leqq Z \leqq 1$) by Eq. 1 using the traces for 1 min (75,000 data points).

# RESULTS

## Simultaneous measurement of the rotation of multiple flagellar motors

We simultaneously measured the rotation of motors of individual *E. coli* cells that were normal-sized and well energized (11) by combining a high-speed camera (1250 frames/s) and the bead assay method described in our previous studies (12–14) (Fig. 1 *A*). A polystyrene bead was attached to each of the sticky flagellar filaments (7). The spatial resolution of our measurement system was confirmed to be 1 nm, which corresponds to an angular resolution of 0.3° of motor rotation. A representative image is shown in the left panel of Fig. 1 *B*, in which two cells, one with two motors (motors 1 and 2) and the other with one motor (motor 3) that are labeled by beads, are observed side by side. The rotational motion of each bead was recorded sequentially (Fig. 1 *C*), and the rotational speed and direction was calculated by the procedure described in Materials and Methods. These cells also express a GFP-fused form of the chemotaxis protein CheW, which is associated with chemoreceptors. The fluorescence image in the right panel of Fig. 1 *B* indicates the position of the GFP-CheW cluster in each cell, which represents the position of the chemoreceptor patch.

## Coordinated switching of the rotation of two motors on the same cell

The rotational motion of each bead was analyzed to obtain the time trace of the rotational speed and directional switching of the motor, as shown in Fig. 2 *A*. Motor 1 (*red trace* in the *upper panel* of Fig. 2 *A*) and motor 2 (*blue* in the *middle*), which were on the same cell, often showed coordinated switching in their rotational direction both from CCW to CW (CCW-to-CW switching) and from CW to CCW (CW-to-CCW switching), but the switching of motor 3 on the other cell showed no coordination with either motor 1 or 2 (see also Movie S1 in the Supporting Material). To verify the coordination of the switching between motors 1

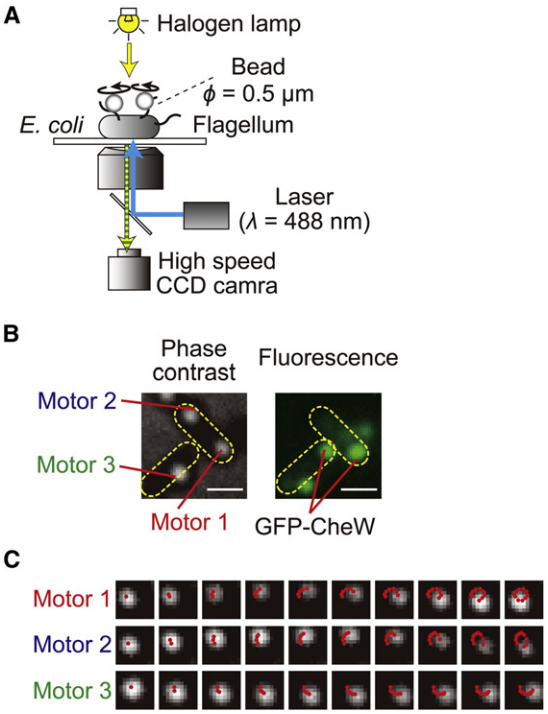


FIGURE 1 Rotational behavior of multiple flagellar motors and intracellular localization of GFP-CheW. (*A*) Schematic diagram of the measurement system. The cell was stuck to a coverslip, and polystyrene beads ($\phi = 0.5\ \mu$m) were attached to the sticky flagellar stubs. The phase-contrast image of each bead was recorded with a high-speed CCD camera (1250 frames/s). By calculating the angular velocity from the position of each bead, the rotational speed and direction could be estimated. A blue laser beam was focused on the back focal plane of the objective lens to excite the GFP-CheW. (*B*) Phase-contrast image of the cells and beads (*left*) and fluorescence image of the cells (*right*). Bar, 1.0 $\mu$m. The yellow-dotted ellipses indicate the cell bodies, motors 1 and 2 on the same cell, and motor 3 on a different cell. The strain used for the measurements had a wild-type *cheW* and a *gfp-cheW* gene encoded in chromosome and plasmid, respectively. Therefore, both wild-type CheW and GFP-CheW were coexpressed in this strain. (*C*) Rotational motions of three motors. Phase contrast images of beads were shown every 0.8 ms. The beads depicted by motors 1, 2, and, 3 correspond to the motors shown in Fig. 1 *B*. Red points on the image of beads indicate the centers of beads every 0.8 ms.

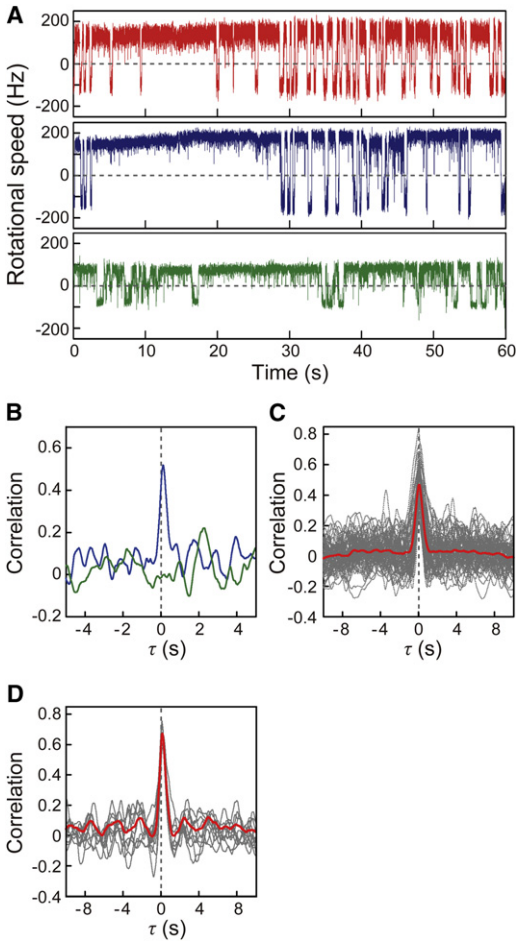


FIGURE 2 Correlation analysis of the switching between two motors. (*A*) The time courses of the rotational speeds of motor 1 (*red*), 2 (*blue*), and 3 (*green*), which are depicted in Fig. 1 *B*. The plus and minus values represent CCW and CW rotations, respectively. (*B*) Correlation analyses between motors 1 and 2 (*blue line*), and between motors 1 and 3 (*green line*), which are depicted in Fig. 2 *A*. Analyses were made based on motor 1. Correlations ($Z(\tau)$) were calculated ($-1 \leqq Z \leqq 1$) using Eq. 1 (see Materials and Methods). (*C*) Gray lines indicate an individual correlation analysis for cells (64 cells) and red line indicates the average trace of the correlation analyses from these cells. (*D*) Correlation of data measured for 10 min (*red line*) and the 1 min-subsets (*gray lines*) for a single *E. coli* cell.

and 2 on the same cell, a correlation analysis was performed as described in Materials and Methods, and the Supporting Material (Fig. S1). The analysis showed a major peak with a time delay of nearly 0 s (Fig. 2 *B*, *blue line*) followed by subsequent minor peaks. In contrast, the correlation analysis between motors 1 and 3 showed no significant peaks (Fig. 2 *B*, *green line*).

A correlation analysis was performed on 1-min time traces of two motors (on the same cell) obtained from 68 cells, and the near-0-s peak was detected in 64 of the cells (94%). The near 0-s peak was still apparent in the averaged correlation profile (Fig. 2 *C*, *red line*) for the data obtained from the 64 cells (*gray line*); however, the minor peaks all averaged each other out, indicating that only the near-0-s peak was meaningful. Essentially the same results were obtained using a 10-min-long trace for a single *E. coli* cell; the near-0-s peak was still apparent, with smaller minor peaks than those seen in the 1-min subsets (Fig. 2 *D*). Therefore, the high degree of coordination of the rotational switching is a general feature of the multiple flagellar motors on a single bacterial cell.

## Correlation analysis of motor switching in a cell constitutively expressing an active CheY mutant or a mutant cell with the *cheZ* gene deleted

To determine whether the coordinated switching between motors was dictated by the signal (CheY-P) produced by

the chemoreceptors, we investigated the correlation of motor switching in cells expressing a constitutively active CheY mutant (caCheY) with Asp-13 replaced with lysine (15). The caCheY mimics the CW-rotation-stimulating function of CheY-P. However, because it does not depend on phosphorylation by the chemoreceptors for its activity, the signaling molecules should be distributed uniformly throughout the cell. In the cell expressing caCheY shown in Fig. 3, *A* and *B*, no coordination was detected in the switching of two motors, and the same was true for all other cells expressing caCheY that we tested (Fig. 3 *C*). Any interaction between the flagellar motor and CheY-P generated by chemoreceptors would be inhibited by the caCheY that was distributed uniformly throughout the cell. This result thus suggests that the coordinated switching between motors is dictated by CheY-P.

We also measured the switching of multiple motors in a deletion mutant of the *cheZ* gene, which encodes the phosphatase for CheY-P, and again observed a lack of coordination in the switching of two motors (Fig. 4, *A* and *B*). The same result was obtained in for all the *cheZ*-deleted cells examined (Fig. 4 *C*). The coordination could be restored by complementation by CheZ expressed from a plasmid (Fig. 4, *D–F*). This result indicated that CheZ is required for the coordinated switching between motors. Therefore,

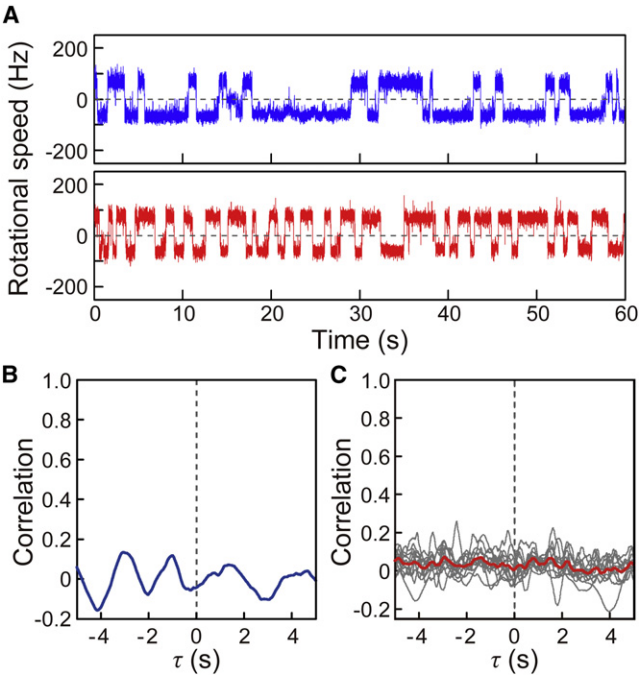


FIGURE 3 Correlation analysis in cells expressing constitutively active CheY mutant. (*A*) The time courses of the rotational speeds of two motors of a cell expressing constitutively active CheY mutant. (*B*) Correlation analysis for the switching between the two motors shown in Fig. 3 *A*. (*C*) Individual correlation analyses performed on 10 cells expressing constitutively active CheY mutant (*gray lines*) and the average trace of the correlation analyses from these cells (*red line*).

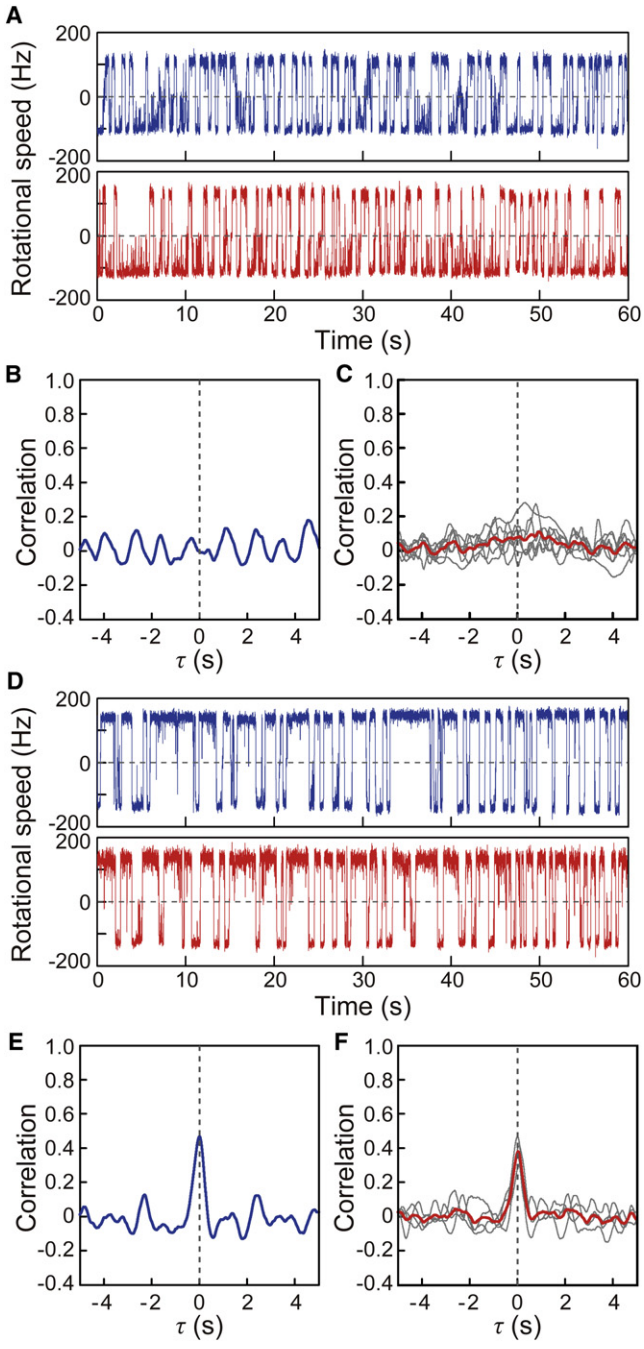


FIGURE 4 Correlation analysis in a *cheZ* deletion mutant. (*A*) Time courses of the rotational speeds of two motors of the *cheZ*-deleted cell. (*B*) Correlation analysis for the switching between the two motors shown in Fig. 4 *A*. (*C*) Individual correlation analyses performed on seven cells in which the *cheZ* gene was deleted (*gray lines*) and the average trace of the correlation analyses from these cells (*red line*). (*D*) Time courses of the rotational speeds of two motors of *cheZ*-deleted cell in which CheZ protein was expressed from a plasmid. (*E*) Correlation analysis for the switching between the two motors shown in Fig. 4 *D*. The $\Delta\tau$ value is 5 ms. (*F*) Individual correlation analyses performed on four *cheZ*-deleted cells in which the CheZ protein was expressed from a plasmid (*gray lines*) and the average trace of the correlation analyses from these cells (*red line*). The $\Delta\tau$ values for four cells are 5, 7, 66, and 70 ms, respectively.

the coordinated switching of multiple motors on a single cell appears to depend on transient changes in the concentration of CheY-P generated by the chemotactic system.

## Relationship between the distance of a motor from the chemoreceptor patch and the delay in switching

Fig. 5 *A* shows the sequential images of two beads attached to flagellar filaments taken from Fig. 1 *B* (motors 1 and 2). In the CCW-to-CW switching, motor 1, which was closer to the chemoreceptor patch (0.14 $\mu$m from the patch), preceded motor 2, which was farther away from the patch (1.5 $\mu$m from the patch), for ~50 ms (see also Fig. S2). Fig. 5 *B* shows the first 3 s of the switching behavior of motors 1 and 2 taken from Fig. 2 *A*, in which all switching events of motor 1 preceded motor 2 (see also Movie S1). Fig. 5 *C* shows a magnified version of the correlation profile shown in Fig. 2 *B*. The peak (*red arrow* for the *blue line*) occurred at a delay time ($\Delta\tau$) of +116 ms, which was consistent with the difference in the delay time between the switching of motors 1 and 2 (Fig. 5 *B*). When the correlation profile was calculated for the CCW-to-CW switching and the CW-to-CCW switching individually, the correlation and similar values of $\Delta\tau$ were detected (data not shown).

To quantify the relationship between the delay time and the distance of the two motors from the chemoreceptor patch, the $\Delta\tau$ value was plotted against $M2^2 - M1^2$, where $M1$ and $M2$ were the distances from the chemoreceptor patch to the closer motor and to the further motor of the two motors, respectively. The $\Delta\tau$ value increased with increasing $M2^2 - M1^2$ (Fig. 5 *D*, *solid circles*). A similar tendency was observed for cells lacking GFP-CheW (Fig. 5 *D*, *open squares*), for which the position of the chemoreceptor patch was assumed so that $\Delta\tau$ had a positive value, because the chemoreceptor patch was not fluorescently labeled in these cells.

The average diffusion coefficient estimated from each plot of $\Delta\tau$ versus $M2^2 - M1^2$ was 11.7 $\pm$ 3.1 (mean $\pm$ SE, $n = 48$) $\mu m^2/s$ (see Eq. S2 in the Supporting Material). This estimated value is consistent with previous reports: 10 $\mu m^2/s$ (CheY) (16) and 4.6 $\mu m^2/s$ (CheY-GFP) (17). This finding suggests that the signal molecules (CheY-P) are propagated from the chemoreceptor patch localized at the cell pole. Therefore, it appears that the $\Delta\tau$ value reflects the time required for the CheY-P molecules to propagate from the chemoreceptor patch to each motor. The linear regression line does not extrapolate to the origin (Fig. 5 *D*). This might be explained by the difference of diffusion coefficient in each cytoplasmic region or the interaction of CheY-P molecules with other intracellular components.

## Simultaneous measurement of the rotation of multiple flagellar motors in an artificial filamentous cell

To investigate how far the signals could travel from the chemoreceptors through the cytoplasm, we measured the switching of motors on a cell that was artificially elongated by cephalexin (Fig. 6 *A*, *top image*). The near 0-s peak was detected in the switching between motors 3 and 4, which were located close to each other (0.7 $\mu$m). However, there was no significant peak for any pairwise combinations of flagella that were 2.2–6.8 $\mu$m away from each other (Fig. 6 *B*). In addition, in the filamentous cells, many fluorescent spots derived from GFP-CheW were randomly

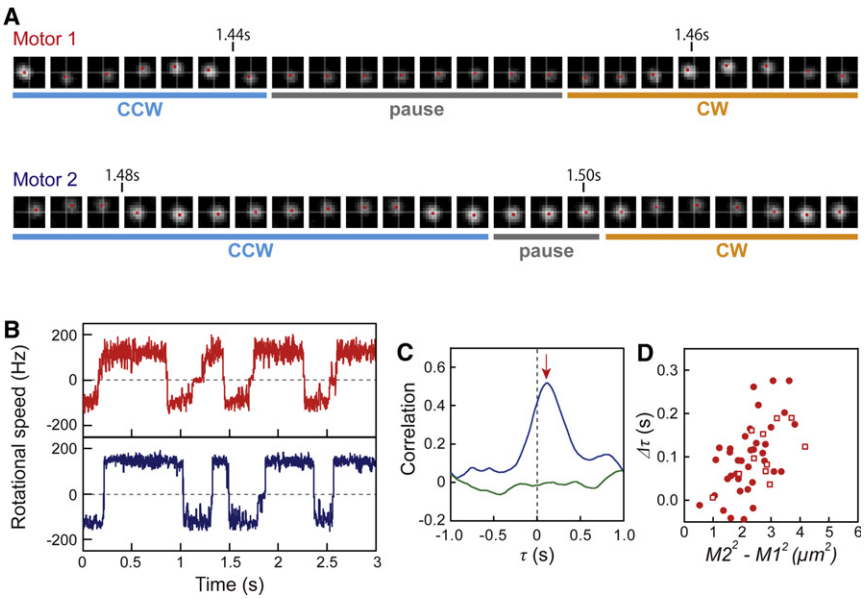


FIGURE 5 Delay of switching in the motor dependent on the distance from the chemoreceptor patch. (*A*) Sequential images of two beads attached to flagellar filaments on the same cell. The time shown on the images corresponds to Fig. 5 *B*. Motors 1 and 2 are the same ones shown in Fig. 1 *B*. Images are shown every 1.6 ms. (*B*) The rotational behavior of motors 1 (*red*) and 2 (*blue*), shown in Fig. 2 *A*, over a short time period. (*C*) Magnified traces of the correlation analyses shown in Fig. 2 *B*. The red arrow for the blue line indicates the peak of correlation (+116 ms). (*D*) The relationship between the $\Delta\tau$ value and $M2^2 - M1^2$. In cells expressing GFP-CheW ($n = 37$), the correlation analyses were made based on the motor closest to the major chemoreceptor patch (*circles*). To evaluate the propagation of CheY-P, cells with a monopolar localization of GFP-CheW and/or cells showing fluorescence at one cell pole that was obviously stronger than at the other pole were chosen. In the cells without GFP-CheW ($n = 11$), the position of the chemoreceptor patch was assumed so that $\Delta\tau$ had a positive value, because the chemoreceptor patch was not fluorescently labeled (*squares*).

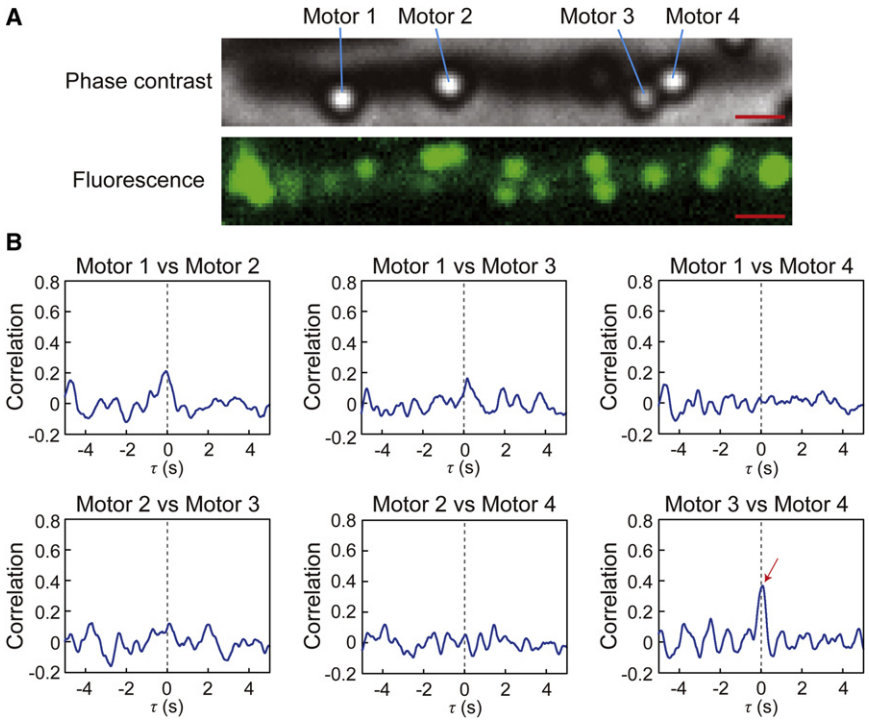


FIGURE 6 Correlation analysis in an artificial filamentous cell. (*A*) The phase-contrast image of an artificial filamentous cell and beads (*top*) and the fluorescence image of this cell (*bottom*). Motors 1, 2, 3, and 4 represent bead-labeled flagellar motors whose rotation could be analyzed. In this filamentous cell, many fluorescent spots (>10) derived from GFP-CheW were randomly distributed along the length of the cell. This observation indicated that there were many lateral chemoreceptor patches in the cell. Bar, 1.0 $\mu$m. (*B*) Correlation analyses for the switching between each pair of flagellar motors. Red arrow indicates near-0-s peak of correlation. The distances between motors 1 and 2, 1 and 3, 1 and 4, 2 and 3, 2 and 4, and 3 and 4 were 2.2, 6.2, 6.8, 4.1, 4.7, and 0.7 $\mu$m, respectively.

distributed along the length of the cells (Fig. 6 *A*, *bottom image*), indicating that there were many lateral chemoreceptor patches in the filamentous cell. Thus, it was possible that the correlation was not detected between the motors separated by greater distances because of both the decay of the signal by diffusion and the disordered signal generated by signal molecules released by the additional lateral chemoreceptor patches on the filamentous cell.

## DISCUSSION

By measuring the rotational motion of multiple flagellar motors simultaneously, we obtained the following results:

1. The motors on the same cell coordinately switch their rotational direction.
2. The coordinated switching is dictated by the intracellular signaling molecule, CheY-P.
3. The dephosphorylation of CheY-P by CheZ is required for the coordinated switching.
4. In both CCW-to-CW and CW-to-CCW switching, the motor that is closer to the chemoreceptor patch switches earlier than another motor farther from it.
5. The delay time of switching ($\Delta\tau$) between two motors increased with the difference between the squared distance of each motor from the chemoreceptor patch ($M2^2 - M1^2$).

Results 1–3 suggest that the change in the CheY-P concentration directly triggers the coordinated switching of the rotational direction of the motors. Cluzel et al. (17) reported that the CW bias is drastically changed above a certain concentration (threshold) of CheY-P. If the CheY-P concentration in the cell temporally changes above and below a threshold, the rotational direction of multiple motors would switch coordinately from CCW to CW, and vice versa. From the delay time of switching $\Delta\tau$ (result 4) and the relationship between $\Delta\tau$ and $M2^2 - M1^2$ (result 5), we propose that CheY-P is predominantly produced intermittently and diffuses from the chemoreceptor patch localized at one of the cell poles, and that the transient change in the CheY-P concentration is propagated to each motor with a delay time that correlates with the distance of the motor from the chemoreceptor patch. Therefore, the multiple motors coordinately switch their rotational direction in response to transient increases and decreases in the CheY-P concentration propagated from the chemoreceptor patch.

Our observations showed that the motor closer to the chemoreceptor patch preceded another motor farther from it in both CCW-to-CW and CW-to-CCW switching. This result could not be explained by only simple diffusion of CheY-P from the receptor patch. If the CheY-P molecules propagated by simple diffusion from the cell pole, the concentration of CheY-P around a motor closer to chemoreceptor patch would always be higher than the concentration around another motor farther from it. In this case, the CCW-to-CW switching of the motor closer to the patch precedes that of another motor father from it; however, the CW-to-CCW switching of a motor closer to the patch would be delayed compared to that of another motor farther away. This is inconsistent with our observation for the CW-to-CCW

switching. To explain our result, we have to suppose that the dynamic changes in the CheY-P concentration, such as sudden increase or decrease, occur around a motor closer to the chemoreceptor patch first, and the change then follows similarly around the motor farther away (Fig. 7).

It is most likely that a wave of CheY-P concentration moves down the cell and reaches each motor at a different time. To produce this kind of change in the CheY-P concentration, the going-up and -down of kinase activity of CheA and the diffusion of CheY-P molecules are insufficient. Therefore, we must consider the involvement of additional factors. One such candidate is CheZ, which is localized at the chemoreceptor patch via the short form of CheA

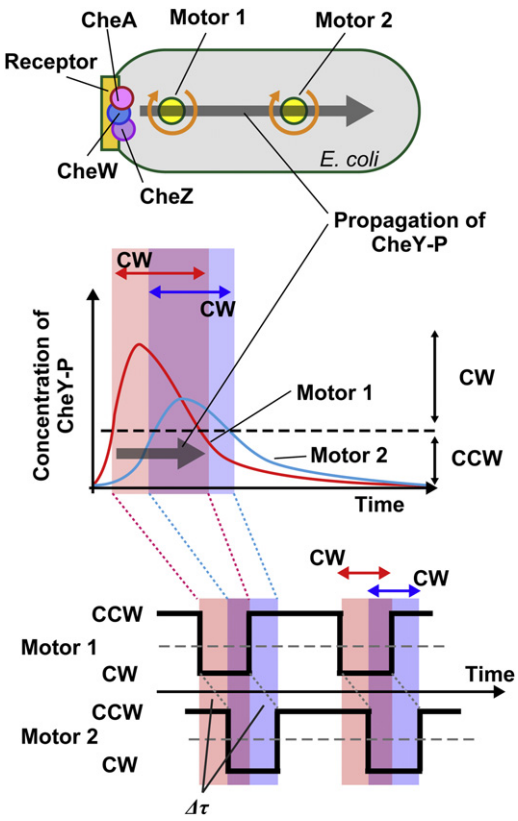


FIGURE 7 Model of intracellular signaling. The receptor patch, including chemoreceptor, histidine kinase CheA, phosphatase CheZ, and CheW is localized at the left side of *E. coli* cell. Motor 1 is the closest to the chemoreceptor patch, and motor 2 is the farthest from it (*top*). A transient increase and decrease in the concentration of a signal protein (CheY-P) from the chemoreceptor patch, which is probably a wavelike change in under a second, triggers and regulates the coordinated switching of flagellar motors. The intracellular signaling molecules were generated at the chemoreceptor patch and propagated toward to another cell pole. The concentration of CheY-P above the threshold for switching increases around motor 1 first, and the increasing then follows around motor 2. In addition, the decreasing of concentration of CheY-P around motor 1 precedes that of around motor 2 (*middle*). In this case, motor 1 closest to the chemoreceptor patch precedes motor 2 farthest from it in switching CCW-to-CW and CW-to-CCW (*bottom*). The phosphatase activity of CheZ as well as the diffusion of CheY-P molecules would be important to produce a wavelike change in the CheY-P concentration.

(18–21). Thus, CheY and CheY-P would be phosphorylated and dephosphorylated at the receptor patch, respectively. We showed that the presence of CheZ is required for the coordinated switching between the motors on a cell (Fig. 4). Therefore, the position and phosphatase activity of CheZ, in addition to the diffusion of CheY-P molecules from a cell pole within a closed compartment of the cell, are likely to be required to produce the wave of CheY-P concentration from the cell pole.

The observed coordinated switching with delays between motors might be explained even if the CW-to-CCW switching does not occur by the decrease of the CheY-P concentration and occurs stochastically with a much longer time constant, whereas the CCW-to-CW switching is caused by the increased CheY-P concentration. In this case, increased levels of CheY-P would be propagated like a short pulse wave, with the duration of CheY-P concentration above the threshold being shorter than the duration of the CW rotation. The CW-to-CCW switching is therefore caused by a relatively slow stochastic dissociation of CheY-P from the motor after the decrease of CheY-P concentration. To create a pulse wave of CheY-P concentration, a rapid decrease in CheY-P by the phosphatase activity of CheZ might also be required. We do not know which model reflects the mechanism for coordinated switching, because we have not observed the propagation of CheY-P molecules directly.

The switching of the flagellar motors in a single cell was investigated previously, but it was reported not to be coordinated in switching (22,23). The primary reasons for the conflicting results obtained by the earlier studies and ours are the mutant *E. coli* cells used and the much lower spatial and temporal resolutions of the earlier experiments. In the study by Macnab and Han (22), the measurements were performed with mutant motors that showed a high intrinsic CW bias, and the rotation of the motors was slowed by oxygen depletion and observed at 1-s intervals. In the study of Ishihara et al. (23), the correlation analysis was performed for two motors far apart on filamentous cells (3–47 $\mu$m), in which the intracellular signal would have decayed by the diffusion of signal molecules over the long distance between the two motors and disordered by signal molecules released from many chemoreceptor patches in the filamentous cell.

By measuring the directional switching of multiple flagellar motors on a single cell, we demonstrated the coordinated control of multiple locomotive organelles via the diffusion of an intracellular signal from a localized chemoreceptor patch. In other words, we were able to measure for the first time, to our knowledge, the dynamic behaviors of the CheY-P signal, in its activation by the chemoreceptor patch, inactivation by CheZ, and its diffusion within the cell. In our experiments, the motors in a cell frequently changed their rotational direction in a coordinated manner, even though no attractant or repellent stimulus was present.

Thus, the receptor patch seems to produce signals spontaneously, as reported previously (24), and the signals appear in bursts by the coordinated regulation of chemoreceptor complexes to generate a wave of signal.

Studies by Turner et al. (25) and Vladimirov et al. (26) showed that the angular change in the swimming direction during a tumble becomes greater when a larger fraction of flagellar filaments in a bundle switch to CW rotation. Thus, the transient increase and decrease in the concentration of CheY-P, which is probably a wavelike change that propagates in under a second from the chemoreceptor patch, may trigger and regulate the coordinated switching of multiple flagellar motors to control the degree of the angular change in the swimming direction in the chemotactic system of *E. coli*.

The basic mechanisms of signal transduction networks are shared not only by bacterial chemotactic systems but also by many organisms, including eukaryotes (1–4). Our findings provide insight into the mechanism of the coordinated switching of multiple flagellar motors by a signal transduction system in prokaryotic cells, as well as what we believe to be a novel perspective on the dynamic behaviors of more complex signal transduction networks.

## SUPPORTING MATERIAL

Additional materials and methods, one table, two figures, and a movie are available at http://www.biophysj.org/biophysj/supplemental/S0006-3495(11)00378-X.

We thank Profs. Michael Manson and Keiichi Namba for their critical reading of this manuscript; Prof. Ikuro Kawagishi, Dr. Yoshiyuki Sowa, and Dr. Takehiko Inaba (at Hosei University) for plasmids; and Dr. Tatsuo Shibata and Dr. Masatoshi Nishikawa (at RIKEN) for useful discussions.

This work was supported by Grants-in-Aid for Scientific Research from the Ministry of Education, Culture, Sports, Science and Technology and from the Japan Society for the Promotion of Science (to H.F. and A.I.).

## REFERENCES

1. Maeda, T., S. M. Wurgler-Murphy, and H. Saito. 1994. A two-component system that regulates an osmosensing MAP kinase cascade in yeast. *Nature.* 369:242–245.
2. Schuster, S. C., A. A. Noegel, …, M. I. Simon. 1996. The hybrid histidine kinase DokA is part of the osmotic response system of *Dictyostelium*. *EMBO J.* 15:3880–3889.
3. Wilkinson, J. Q., M. B. Lanahan, …, H. J. Klee. 1995. An ethylene-inducible component of signal transduction encoded by never-ripe. *Science.* 270:1807–1809.
4. Wadhams, G. H., and J. P. Armitage. 2004. Making sense of it all: bacterial chemotaxis. *Nat. Rev. Mol. Cell Biol.* 5:1024–1037.
5. Darnton, N. C., L. Turner, …, H. C. Berg. 2007. On torque and tumbling in swimming *Escherichia coli*. *J. Bacteriol.* 189:1756–1764.
6. Parkinson, J. S., and S. E. Houts. 1982. Isolation and behavior of *Escherichia coli* deletion mutants lacking chemotaxis functions. *J. Bacteriol.* 151:106–113.
7. Ryu, W. S., R. M. Berry, and H. C. Berg. 2000. Torque-generating units of the flagellar motor of *Escherichia coli* have a high duty ratio. *Nature.* 403:444–447.
8. Datsenko, K. A., and B. L. Wanner. 2000. One-step inactivation of chromosomal genes in *Escherichia coli* K-12 using PCR products. *Proc. Natl. Acad. Sci. USA.* 97:6640–6645.
9. Maloy, S. R., and W. D. Nunn. 1981. Selection for loss of tetracycline resistance by *Escherichia coli*. *J. Bacteriol.* 145:1110–1111.
10. Chung, S. H., and R. A. Kennedy. 1991. Forward-backward non-linear filtering technique for extracting small biological signals from noise. *J. Neurosci. Methods.* 40:71–86.
11. Inoue, Y., C. J. Lo, …, A. Ishijima. 2008. Torque-speed relationships of $Na^+$-driven chimeric flagellar motors in *Escherichia coli*. *J. Mol. Biol.* 376:1251–1259.
12. Sowa, Y., A. D. Rowe, …, R. M. Berry. 2005. Direct observation of steps in rotation of the bacterial flagellar motor. *Nature.* 437:916–919.
13. Fukuoka, H., Y. Sowa, …, M. Homma. 2007. Visualization of functional rotor proteins of the bacterial flagellar motor in the cell membrane. *J. Mol. Biol.* 367:692–701.
14. Fukuoka, H., Y. Inoue, …, A. Ishijima. 2010. Exchange of rotor components in functioning bacterial flagellar motor. *Biochem. Biophys. Res. Commun.* 394:130–135.
15. Bourret, R. B., J. F. Hess, and M. I. Simon. 1990. Conserved aspartate residues and phosphorylation in signal transduction by the chemotaxis protein CheY. *Proc. Natl. Acad. Sci. USA.* 87:41–45.
16. Segall, J. E., A. Ishihara, and H. C. Berg. 1985. Chemotactic signaling in filamentous cells of *Escherichia coli*. *J. Bacteriol.* 161:51–59.
17. Cluzel, P., M. Surette, and S. Leibler. 2000. An ultrasensitive bacterial motor revealed by monitoring signaling proteins in single cells. *Science.* 287:1652–1655.
18. Lipkow, K., S. S. Andrews, and D. Bray. 2005. Simulated diffusion of phosphorylated CheY through the cytoplasm of *Escherichia coli*. *J. Bacteriol.* 187:45–53.
19. Sourjik, V., and H. C. Berg. 2000. Localization of components of the chemotaxis machinery of *Escherichia coli* using fluorescent protein fusions. *Mol. Microbiol.* 37:740–751.
20. Cantwell, B. J., and M. D. Manson. 2009. Protein domains and residues involved in the CheZ/$CheA_S$ interaction. *J. Bacteriol.* 191:5838–5841.
21. Vaknin, A., and H. C. Berg. 2004. Single-cell FRET imaging of phosphatase activity in the *Escherichia coli* chemotaxis system. *Proc. Natl. Acad. Sci. USA.* 101:17072–17077.
22. Macnab, R. M., and D. P. Han. 1983. Asynchronous switching of flagellar motors on a single bacterial cell. *Cell.* 32:109–117.
23. Ishihara, A., J. E. Segall, …, H. C. Berg. 1983. Coordination of flagella on filamentous cells of *Escherichia coli*. *J. Bacteriol.* 155:228–237.
24. Borkovich, K. A., N. Kaplan, …, M. I. Simon. 1989. Transmembrane signal transduction in bacterial chemotaxis involves ligand-dependent activation of phosphate group transfer. *Proc. Natl. Acad. Sci. USA.* 86:1208–1212.
25. Turner, L., W. S. Ryu, and H. C. Berg. 2000. Real-time imaging of fluorescent flagellar filaments. *J. Bacteriol.* 182:2793–2801.
26. Vladimirov, N., D. Lebiedz, and V. Sourjik. 2010. Predicted auxiliary navigation mechanism of peritrichously flagellated chemotactic bacteria. *PLOS Comput. Biol.* 6:e1000717.